Parametric Localization of Distributed Sources

Shahrokh Valaee, Benoit Champagne, *Member, IEEE,* and Peter Kabal, *Member, IEEE*

***Abstract*—Most array processing algorithms are based on the assumption that the signals are generated by point sources. This is a mathematical constraint that is not satisfied in many applications. In this paper, we consider situations where the sources are distributed in space with a parametric angular cross-correlation kernel. We propose an algorithm that estimates the parameters of this model using a generalization of the MUSIC algorithm. The method involves maximizing a cost function that depends on a matrix array manifold and the noise eigenvectors. We study two particular cases: coherent and incoherent spatial source distributions. The spatial correlation function for a uniformly distributed signal is derived. From this, we find the array gain and show that (in contrast to point sources) it does not increase linearly with the number of sources. We compare our method to the conventional (point source) MUSIC algorithm. The simulation studies show that the new method outperforms the MUSIC algorithm by reducing the estimation bias and the standard deviation for scenarios with distributed sources. It is also shown that the threshold signal-to-noise ratio required for resolving two closely spaced distributed sources is considerably smaller for the new method.**

I. Introduction

In ARRAY processing it is frequently assumed that the signals of interest are generated by far-field point sources. Many practical examples can be found where the point source assumption does not hold. For instance, in an undersea echo beam sounder, penetration of the transmitted pulse into the seabed and scattering on the lower layers creates a spatial distribution of energy at the receiving array that is equivalent to a superposition of plane waves originating from a continuum of directions [1]. Such apparent distributed sources also appear in the application of a microphone array to the localization of acoustic sources in a highly reverberant room [2]. In tropospheric or ionospheric propagation of radio waves, scattering causes the receiver to see a distributed source [3]. Also, low-elevation radio links are subject to ground reflections resulting in distributed signal components [4]. Similarly, multipath propagation in indoor mobile radio communications affects the observed signal spatial distribution [5]. Depending on the nature of the reflection and scattering in the above examples, signal components arriving from different directions exhibit varying degrees of correlation, ranging from totally uncorrelated (incoherent) to fully correlated (coherent) cases.

For narrowband point-source configurations, the dimension of the signal subspace (defined as the span of the correlation matrix in a noise-free environment) is equal to the number of noncoherent signals. Thus, each source has a 1-D representation in the signal subspace. A distributed source can be viewed as a combination of a multitude of closely spaced point sources. If the point sources are treated as being independent, the corresponding location matrix spans the whole space and the noise subspace is empty. This explains why conventional array processing techniques such as MUSIC [6] and ESPRIT [7], which are based on the signal and noise subspace decomposition for point source scenarios, often lead to erroneous results when directly applied to distributed source localization [1].

Despite its importance, the literature on distributed source localization is sparse. Jäntti [1] models a distributed source with a finite number of point sources. Then, he uses the traditional MUSIC or ESPRIT algorithms to localize those point sources. The drawback is that for unique localization, the maximum number of point sources should be upper bounded by the number of sensors [8]. Moreover, it is not clear how the point source location estimates can be used to infer about the spatial distribution of an extended source. In [9], a maximum likelihood (ML) approach to distributed source localization has been considered. The likelihood function is jointly maximized for all parameters of a model with Gaussian source distribution. The complexity of this method grows exponentially with the number of unknown parameters. A discrete modeling approach has been taken in [10] for nonoverlapping sources. There, each distributed source is modeled by a number of point sources (150–200 is suggested) resulting in an array of the same dimensionality. To circumvent the problem of unique localization, it is assumed that the parameterized shape of the distribution is known.

In this paper, we describe a new high-resolution technique for the localization of distributed narrowband sources, which was first proposed in [11]. The method is computationally efficient and does not rely on a decomposition of distributed sources into clusters of closely spaced point sources. In our approach, the spatial correlation of the distributed signal is assumed to belong to a class of positive-definite functions, each function being uniquely characterized by a parameter vector. Under this assumption, the localization problem reduces to one of parameter estimation. The noise-free observation vector is modeled as the image of the source signal through a linear operator. The adjoint of this operator is used to transform properly defined noise eigenvectors into an appropriate source subspace. The parameter vector is then

Manuscript received November 12, 1993; revised December 5, 1994. This work was supported in part by a grant from the Natural Sciences and Engineering Research Council of Canada (NSERC). The associate editor coordinating the review of this paper and approving it for publication was Dr. Athina Petropulu.

S. Valaee is with the INRS-Télécommunications, Université du Québec, Verdun, Québec, Canada H3E 1H6.

B. Champagne is with the INRS-Télécommunications, Université du Québec, Verdun, Québec, Canada H3E 1H6.

P. Kabal is with the Department of Electrical Engineering, McGill University, Montréal, Québec, Canada H3A 2A7 and the INRS-Télécommunications, Université du Québec, Verdun, Québec, Canada H3E 1H6.

IEEE Log Number 9413324.

estimated by minimizing a certain norm of the transformed noise eigenvectors. The proposed localization method is based on a generalization of the MUSIC algorithm and is applicable to distributed sources with a wide range of spatial correlation structures. In the paper, we specialize the new method to two particular types of distributed sources, namely: coherently distributed (CD) and incoherently distributed (ID) sources. For a CD source, the signal components arriving from different angles within the extension width are coherent (fully correlated). For an ID source, these components are uncorrelated.

The new method has been simulated and compared to the conventional MUSIC algorithm. The results show a dramatic improvement in performance for the new algorithm for distributed sources. In particular, the new method has a smaller variance and, unlike MUSIC, it is asymptotically unbiased. The threshold signal-to-noise ratio (SNR) required for resolving two closely spaced distributed sources is also considerably smaller. Furthermore, the new method has the advantage of providing information about the spatial extension of the sources.

The paper is organized as follows. In the following section, we formulate the problem and classify the distributed sources in terms of their spatial correlation functions. In Section III, we develop the new parameter estimation technique for the localization of distributed sources. This is specialized to the cases of CD and ID sources. In Section IV, we study the shortcomings of the conventional beamforming techniques when applied to distributed sources. In particular, we show that the array gain is bounded and cannot increase linearly with the number of sensors. The computer simulations are presented in Section V. Section VI summarizes our findings.

II. Models for Spatially Distributed Sources

Consider an array of p sensors monitoring a wave field of q spatially distributed narrowband sources in additive background noise. For simplicity, it is assumed that the sensors and the sources are in the same plane. However, the method can be easily extended to the 3-D case. The complex envelope representation of the array output observation vector can be given by

$$\mathbf{x} = \sum_{i=1}^{q} \int_{-(\pi/2)}^{\pi/2} \mathbf{a}(\theta) s_i(\theta; \boldsymbol{\psi}_i)\, d\theta + \mathbf{n} \tag{1}$$

where $\mathbf{a}(\theta)$ is the $p \times 1$ location vector of the array, $s_i(\theta; \boldsymbol{\psi}_i)$ is the *angular signal density* of the ith source in the direction $\theta \in [-\pi/2, \pi/2]$, $\boldsymbol{\psi}_i$ is the unknown parameter vector, and $\mathbf{n}$ is the $p \times 1$ additive noise vector.

The integral in (1) is the response of the array to a linear superposition of wavefronts associated to a continuum of directions θ. The nature of these wavefronts (planar, circular, etc.) is dictated by the choice of the location vector $\mathbf{a}(\theta)$. For example, to obtain a plane wave decomposition, one must use location vectors $\mathbf{a}(\theta)$ corresponding to planar wavefronts. Examples of the parameter vector $\boldsymbol{\psi}_i$ are the two limits of the direction-of-arrival (DOA) for a uniform spatial extension, or the angle of maximum power and the -3 dB extension width for a bell-shaped distribution. Fig. 1 depicts two bell-shape distributed sources located at the angles θ_1 and θ_2 with

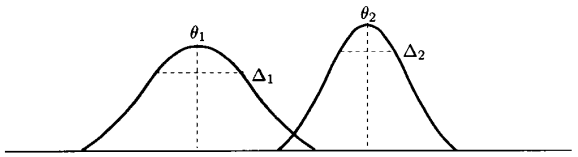

Fig. 1. Two bell-shape distributed sources with spatial overlap located at the angles θ_1 and θ_2 with the -3 dB extension widths Δ_1 and Δ_2.

the -3 dB extension widths Δ_1 and Δ_2. For this example, the parameter vectors are $\boldsymbol{\psi}_1 = (\theta_1, \Delta_1)$ and $\boldsymbol{\psi}_2 = (\theta_2, \Delta_2)$. Note that spatial overlap of the signals is allowed.

Modeling the angular signal densities $s_i(\theta; \boldsymbol{\psi}_i)$ as random variables (for all θ) and the noise $\mathbf{n}$ as a random vector, and assuming that the signal and the noise are uncorrelated, the correlation matrix of the observation vector $\mathbf{x}$ is given by

$$\begin{aligned} \mathbf{R}_x &= E(\mathbf{x}\mathbf{x}^H) \\ &= \mathbf{R}_s(\boldsymbol{\psi}) + \mathbf{R}_n \end{aligned} \tag{2}$$

where $E(\cdot)$ denotes statistical expectation, the superscript H represents Hermitian transposition, $\mathbf{R}_s(\boldsymbol{\psi})$ is the noise-free correlation matrix, and $\mathbf{R}_n$ is the noise correlation matrix. In (2), the noise-free correlation matrix is given by

$$\begin{aligned} \mathbf{R}_s(\boldsymbol{\psi}) = \sum_{i=1}^{q} \sum_{j=1}^{q} \int_{-(\pi/2)}^{\pi/2} \int_{-(\pi/2)}^{\pi/2} \\ \cdot \mathbf{a}(\theta) p_{ij}(\theta, \theta'; \boldsymbol{\psi}_i, \boldsymbol{\psi}_j) \mathbf{a}^H(\theta')\, d\theta\, d\theta' \end{aligned} \tag{3}$$

where

$$p_{ij}(\theta, \theta'; \boldsymbol{\psi}_i, \boldsymbol{\psi}_j) = E[s_i(\theta; \boldsymbol{\psi}_i) s_j^*(\theta'; \boldsymbol{\psi}_j)] \tag{4}$$

and * represents the complex conjugation. We call $p_{ij}(\theta, \theta'; \boldsymbol{\psi}_i, \boldsymbol{\psi}_j)$ the *angular cross-correlation kernel.*

If the signals from different sources are uncorrelated, the angular cross-correlation kernel simplifies to

$$p_{ij}(\theta, \theta'; \boldsymbol{\psi}_i, \boldsymbol{\psi}_j) = p_i(\theta, \theta'; \boldsymbol{\psi}_i)\, \delta_{ij} \tag{5}$$

where δ_{ij} is the Kronecker delta and

$$p_i(\theta, \theta'; \boldsymbol{\psi}_i) = E[s_i(\theta; \boldsymbol{\psi}_i) s_i^*(\theta'; \boldsymbol{\psi}_i)] \tag{6}$$

is the *angular auto-correlation kernel* for source i. The noise-free correlation matrix (3) is then given by

$$\begin{aligned} \mathbf{R}_s(\boldsymbol{\psi}) = \sum_{i=1}^{q} \int_{-(\pi/2)}^{\pi/2} \int_{-(\pi/2)}^{\pi/2} \\ \cdot \mathbf{a}(\theta) p_i(\theta, \theta'; \boldsymbol{\psi}_i) \mathbf{a}^H(\theta')\, d\theta\, d\theta'. \end{aligned} \tag{7}$$

Below, we consider two particular cases of the angular auto-correlation kernel (5) which are of practical interest.

Case I—Coherently Distributed Sources: A source is called *coherently distributed* (CD) if the received signal components from that source at different angles are delayed and scaled replicas of the same signal. In such a case, the angular signal density can be represented as

$$s(\theta; \boldsymbol{\psi}_i) = \gamma_i g(\theta; \boldsymbol{\psi}_i) \tag{8}$$

where γ_i is a random variable and $g(\theta; \boldsymbol{\psi}_i)$ is a complex-valued deterministic function of θ which we call the *deterministic*

angular signal density. Note that a CD signal is decomposable into random and deterministic components. The deterministic component $g(\theta;\boldsymbol{\psi}_i)$, which is parameterized by the vector $\boldsymbol{\psi}_i$, characterizes the spatial distribution of the source, and the random component γ_i reflects the temporal behavior of the source. To motivate the CD model, consider narrowband signal wavefronts reflected by an object and observed by an array of sensors. Under stationary conditions, the signal components reflected from different parts of the object differ by a deterministic phase component that depends on the reflection coefficients of the surface elements, the difference in travel times, and the frequency of the incident wave. Such a reflector can be modeled as a CD source with the phase differences of the received signal components modeled by a deterministic angular signal density $g(\theta;\boldsymbol{\psi}_i)$. From (8), the angular auto-correlation kernel for a CD signal can be represented by

$$p(\theta,\theta';\boldsymbol{\psi}) = \eta g(\theta;\boldsymbol{\psi}) g^*(\theta';\boldsymbol{\psi}) \tag{9}$$

with

$$\eta = E[\gamma\gamma^*]. \tag{10}$$

Case II—Incoherently Distributed Signal: In some applications, the signal rays arriving from different directions can be assumed uncorrelated. For example, in the transmission of the radio-waves through tropospheric scatter links, the signal rays reflected from different layers of the troposphere have uncorrelated phases. A similar effect is observed when the signal rays are the reflections from different parts of a rough surface.[0] The angular auto-correlation kernel for such a case is written as

$$p(\theta,\theta';\boldsymbol{\psi}) = p(\theta;\boldsymbol{\psi})\delta(\theta-\theta') \tag{11}$$

where $p(\theta;\boldsymbol{\psi})$ is the angular power density of the source, and $\delta(\theta)$ is the Dirac delta function. A distributed source with the angular auto-correlation kernel (11) is called the *incoherently distributed* (ID) signal. The noise-free array correlation matrix for these signals is shown as

$$\mathbf{R}_s(\boldsymbol{\psi}) = \sum_{i=1}^{q} \int_{-(\pi/2)}^{\pi/2} \mathbf{a}(\theta) p(\theta;\boldsymbol{\psi}_i) \mathbf{a}^H(\theta)\, d\theta. \tag{12}$$

In practice, an intermediate situation might occur that corresponds to a partially correlated signal where the rays of signal arriving from different angles are partially correlated. Partially correlated signals can also be localized using the same method proposed for the ID signal.

At this point, we find it convenient to summarize the assumptions about signal and noise that are used throughout the paper.

(A1) The sources emit narrowband signals and are located at the far-field of the array of sensors.

(A2) The number of sources q is known. In this paper, we only address the localization problem.

[0] According to the Rayleigh criterion, a surface is rough if $h \sin\theta > \lambda/8$, where h is the height of the roughness in the surface, θ is the reflection angle measured from the normal, and λ is the wavelength of the reflected signal.

(A3) For all $i \neq j$, and for all $\theta,\theta' \in [-\pi/2,\pi/2]$, $s_i(\theta;\boldsymbol{\psi}_i)$ and $s_j(\theta';\boldsymbol{\psi}_j)$ are not fully correlated.

(A4) The temporal samples of the angular signal density $s_i(\theta,\boldsymbol{\psi}_i)$ are modeled as independent, zero-mean, complex random variables.

(A5) The samples of the complex envelope of the noise are modeled as independent, zero-mean, complex random variables with a correlation matrix $\mathbf{R}_n$. In the sequel, we will only consider spatially white noise. If $\mathbf{R}_n$ is known, generalization to the nonwhite case is straightforward.

(A6) The signal and noise are uncorrelated from each other.

(A7) The angular auto-correlation kernel of the sources belongs to a known family of positive definite functions $p(\theta,\theta';\boldsymbol{\psi}_i)$. Here, it is assumed that the shape of the function is known; only the parameter vector is unknown.

In this paper, the main objective is to locate distributed signals. The localization is done by estimating the unknown parameter vectors $\boldsymbol{\psi}_i$ of the angular auto-correlation kernel $p(\theta,\theta';\boldsymbol{\psi}_i)$ of each source. In the following section, we propose a localization technique for CD and ID signals.

III. Localization

In this section, we propose a parametric localization technique for distributed sources which is based on *a priori* knowledge of the distribution of the signals (Assumption A7). Specifically, it is assumed that the angular auto-correlation kernel of each signal belongs to a parametric class of functions. With this assumption, the localization of distributed sources is the same as a parameter estimation problem. We use a linear operator formulation of array processing similar to that of [12] to generalize the MUSIC algorithm for the distributed source model. The new algorithm trades off optimality and computational complexity.

A. A Generalization of the MUSIC Algorithm

Let us denote by $L_2[-\pi/2,\pi/2]$ the Hilbert space of all complex-valued square integrable functions defined over the interval $[-\pi/2,\pi/2]$. The inner product and the norm in this space are defined by

$$\langle s_i, s_j\rangle_c = \int_{-(\pi/2)}^{\pi/2} s_i^*(\theta) s_j(\theta)\, d\theta \tag{13}$$

$$\|s_i\|_c = \sqrt{\langle s_i, s_i\rangle_c} \tag{14}$$

where the subscript c refers to the continuous nature of the functions. According to (1), the observation vector $\mathbf{x}$ at the array output can be expressed as

$$\mathbf{x} = \sum_{i=1}^{q} \mathcal{L} s_i(\cdot;\boldsymbol{\psi}_i) + \mathbf{n} \tag{15}$$

where $\mathcal{L}$ is a linear operator that maps $L_2[-\pi/2,\pi/2]$ into a p-dimensional complex observation vector space $\mathbb{C}^p$ according to

$$\mathcal{L}\colon L_2[-\pi/2,\pi/2] \longrightarrow \mathbb{C}^p \tag{16}$$

$$\mathcal{L}s = \int_{-(\pi/2)}^{\pi/2} \mathbf{a}(\theta) s(\theta)\, d\theta. \tag{17}$$

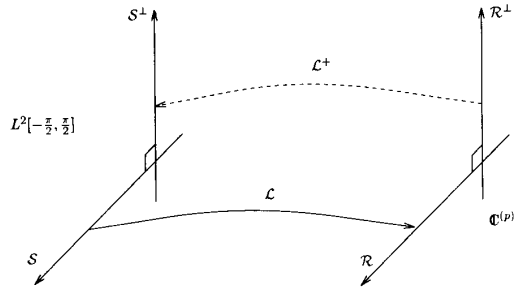

Fig. 2. Geometry of the linear operator and the adjoint operator.

The inner product and the norm in $\mathbb{C}^p$ are defined by

$$\langle \mathbf{x}_i, \mathbf{x}_j \rangle_d = \mathbf{x}_i^H \mathbf{x}_j \tag{18}$$

$$\|\mathbf{x}_i\|_d = \sqrt{\langle \mathbf{x}_i, \mathbf{x}_i \rangle_d} \tag{19}$$

where the subscript d indicates the discrete nature of the functions.

By definition, the adjoint operator $\mathcal{L}^+$: $\mathbb{C}^p \rightarrow L_2[-\pi/2, \pi/2]$ satisfies

$$\langle \mathcal{L}s, \mathbf{x} \rangle_d = \langle s, \mathcal{L}^+ \mathbf{x} \rangle_c. \tag{20}$$

For the linear operator (17), we have

$$\begin{aligned} \langle \mathcal{L}s, \mathbf{x} \rangle_d &= [\mathcal{L}s]^H \mathbf{x} \\ &= \int_{-(\pi/2)}^{\pi/2} s^*(\theta) \mathbf{a}^H(\theta)\, d\theta\, \mathbf{x} \\ &= \langle s, \mathbf{a}^H \mathbf{x} \rangle_c. \end{aligned} \tag{21}$$

Thus, the adjoint is given by

$$\mathcal{L}^+ \mathbf{x} = \mathbf{a}^H(\theta)\mathbf{x}. \tag{22}$$

As a starting point, we extend the definition of the signal and noise subspaces to distributed sources. Note that for a fixed parameter vector ψ_i, the angular signal density $s_i(\theta; \boldsymbol{\psi}_i)$ in (15) is a random process with respect to the DOA parameter θ. By the *source subspace* we mean the linear span of all realizations of the random process $s_i(\theta; \boldsymbol{\psi}_i), i = 1, \cdots, q$, where the $\boldsymbol{\psi}_i$'s are fixed. This subspace is shown by $\mathcal{S}$ and is expressed as

$$\mathcal{S} = \text{Span}\ \{s_i(\theta; \boldsymbol{\psi}_i)\colon i = 1, \cdots, q, \text{and all realizations}\}. \tag{23}$$

For simplicity, we assume that the source subspace $\mathcal{S}$ is a closed subspace of $L_2[-\pi/2, \pi/2]$. However, the theory can be generalized. The range of the linear operator $\mathcal{L}$ under $\mathcal{S}$ is defined as the *signal subspace* and is represented by

$$\mathcal{R} = \{\mathcal{L}s\colon \text{all } s \in \mathcal{S}\}. \tag{24}$$

The orthogonal complement of $\mathcal{R}$ is defined as the *noise subspace* and is denoted by $\mathcal{R}^\perp$. It can be shown that the range of the adjoint operator $\mathcal{L}^+$, when the domain is restricted to the noise subspace $\mathcal{R}^\perp$, is included in the orthogonal complement of $\mathcal{S}$ represented by $\mathcal{S}^\perp$. Fig. 2 schematically depicts the relationship between the linear operators and the subspaces.

The above concept of the signal and noise subspaces can be reconciled with the conventional definitions for the point source case as follows (we temporarily relax the assumption $\mathcal{S} \in L_2[-\pi/2, \pi/2]$). The angular signal density of a point source at the DOA ψ_i can be shown as

$$s_i(\theta; \psi_i) = \gamma_i \delta(\theta - \psi_i) \tag{25}$$

where γ_i is the random complex envelope of the ith signal. According to (23), the source subspace for a point source scenario is given by

$$\mathcal{S} = \text{Span}\{\delta(\theta - \psi_1), \cdots, \delta(\theta - \psi_q)\}. \tag{26}$$

Applying the linear operator $\mathcal{L}$ to (26) gives the signal subspace

$$\mathcal{R} = \text{Span}\{\mathbf{a}(\psi_1), \cdots, \mathbf{a}(\psi_q)\} \tag{27}$$

which corresponds to the conventional definition of the signal subspace for point sources.

We now use the new definitions of the signal and noise subspaces to interpret the conventional MUSIC algorithm for the point sources given in (26). Suppose we know a basis for $\mathcal{R}^\perp$, say $\mathbf{e}_i \in \mathcal{R}^\perp, i = 1, \cdots, p - q$. Then

$$\mathcal{L}^+ \mathbf{e}_i = \mathbf{a}^H(\theta)\mathbf{e}_i \in \mathcal{S}^\perp, \qquad i = 1, \cdots, p - q. \tag{28}$$

Since the back-transformed vector is in the orthogonal complement of $\mathcal{S}$, it is orthogonal to any vector in $\mathcal{S}$

$$\int_{-(\pi/2)}^{\pi/2} \mathbf{a}^H(\theta)\mathbf{e}_i s^*(\theta)\, d\theta = 0 \quad \text{for any } s(\theta) \in \mathcal{S}, \quad \text{and} \quad i = 1, \cdots, p - q. \tag{29}$$

Using (26) we have

$$\int_{-(\pi/2)}^{\pi/2} \mathbf{a}^H(\theta)\mathbf{e}_i \delta(\theta - \psi_j) d\,\theta = \mathbf{a}^H(\psi_j)\mathbf{e}_i = 0, \quad \text{for } i = 1, \cdots, p - q, \quad j = 1, \cdots, q. \tag{30}$$

Defining $\mathbf{E}_n = [\mathbf{e}_1, \cdots, \mathbf{e}_{p-q}]$, we have

$$\mathbf{a}^H(\psi_j)\mathbf{E}_n = \mathbf{0}, \quad \text{for } j = 1, \cdots, q. \tag{31}$$

The MUSIC algorithm estimates the DOA's of multiple point sources by maximizing the following "frequency detector" with respect to the DOA parameter $\psi \in \boldsymbol{\Psi}$, where Θ is the parameter set

$$P_{\text{MUSIC}}(\psi) = \frac{1}{\mathbf{a}^H(\psi)\mathbf{E}_n\mathbf{E}_n^H\mathbf{a}(\psi)} \tag{32}$$

$$= \frac{1}{\|\mathbf{a}^H(\psi)\mathbf{E}_n\|^2}. \tag{33}$$

We use the same approach to derive a MUSIC-type algorithm for the localization of distributed sources. For the moment assume that $\mathcal{R}^\perp$ has dimension $p - q$ and we have a basis for $\mathcal{R}^\perp$, say $\mathbf{e}_1, \cdots, \mathbf{e}_{p-q}$, and let $\mathbf{E}_n = [\mathbf{e}_1, \cdots, \mathbf{e}_{p-q}]$. Since $\mathbf{e}_i$'s are in $\mathcal{R}^\perp$, their image under $\mathcal{L}^+$ will be in $\mathcal{S}^\perp$, i.e.

$$\mathcal{L}^+ \mathbf{e}_i = \mathbf{a}^H(\theta)\mathbf{e}_i \in \mathcal{S}^\perp, \qquad i = 1, \cdots, p - q. \tag{34}$$

Thus, for all $s(\theta) \in \mathcal{S}$ we have

$$\int_{-(\pi/2)}^{\pi/2} \mathbf{a}^H(\theta)\mathbf{E}_n s^*(\theta)\, d\theta = \mathbf{0}. \tag{35}$$

In (23), the source subspace $\mathcal{S}$ was defined as a span of the functions $s_i(\theta;\boldsymbol{\psi}_i)$. Hence, (35) can be written as

$$\int_{-(\pi/2)}^{\pi/2} \mathbf{a}^H(\theta)\mathbf{E}_n s_i^*(\theta;\boldsymbol{\psi}_i)\, d\theta = \mathbf{0} \tag{36}$$

for all realizations of $s_i(\theta;\boldsymbol{\psi}_i)$, and for $i = 1,\cdots,q$. Since $s_i(\theta;\boldsymbol{\psi}_i)$ is a random function, this is equivalent to

$$E\left[\left\|\int_{-(\pi/2)}^{\pi/2} \mathbf{a}^H(\theta)\mathbf{E}_n s_i^*(\theta;\boldsymbol{\psi}_i)\, d\theta\right\|^2\right] = 0, \quad \text{for } i = 1,\cdots,q. \tag{37}$$

Using (6), this equation can be expressed as

$$\int_{-(\pi/2)}^{\pi/2}\int_{-(\pi/2)}^{\pi/2} \mathbf{a}^H(\theta)\mathbf{E}_n p^*(\theta,\theta';\boldsymbol{\psi}_i)\mathbf{E}_n^H\mathbf{a}(\theta')\, d\theta\, d\theta' = 0, \quad i = 1\cdots,q. \tag{38}$$

Following the approach of the point source case leading to (33), we propose that the parameter vector $\boldsymbol{\psi}_i$ of the distributed sources be estimated by locating the peaks of

$$\hat{\boldsymbol{\psi}} = \arg\max_{\boldsymbol{\psi}} \frac{1}{\displaystyle\int_{-(\pi/2)}^{\pi/2}\int_{-(\pi/2)}^{\pi/2} \mathbf{a}^H(\theta)\mathbf{E}_n p^*(\theta,\theta';\boldsymbol{\psi})\mathbf{E}_n^H\mathbf{a}(\theta')\, d\theta\, d\theta'}. \tag{39}$$

This criterion can also be expressed as

$$\hat{\boldsymbol{\psi}} = \arg\max_{\boldsymbol{\psi}} \frac{1}{\operatorname{tr}(\mathbf{E}_n^H\mathbf{H}(\boldsymbol{\psi})\mathbf{E}_n)} \tag{40}$$

where $\operatorname{tr}(\cdot)$ stands for the trace of a matrix and $\mathbf{H}(\boldsymbol{\psi})$ is the matrix array manifold defined by

$$\mathbf{H}(\boldsymbol{\psi}) = \int_{-(\pi/2)}^{\pi/2}\int_{-(\pi/2)}^{\pi/2} \mathbf{a}(\theta)p^*(\theta,\theta';\boldsymbol{\psi})\mathbf{a}^H(\theta')\, d\theta\, d\theta'. \tag{41}$$

We call this method the *distributed signal parameter estimator* (DSPE). To estimate the parameter vector, the spectrum of the DSPE algorithm should be searched in an m-dimensional grid for q prominent local maxima.

If the matrix array manifold is precisely known, the DSPE spectrum can be computed for all parameters in the parameter space. Note that $\mathbf{H}(\boldsymbol{\psi})$ is independent of the observation and hence it can be evaluated and stored prior to computation of the DSPE spectrum. We refer to this step as the calibration process. If the location vector $\mathbf{a}(\theta)$ is known for all θ, calibration amounts to the evaluation of $\mathbf{H}(\boldsymbol{\psi})$ for all $\boldsymbol{\psi}$ of interest. When there are uncertainties in the location vector, the latter should be measured experimentally. Then, the matrix array manifold can be computed using the measured location vectors. Note that the calibration should be implemented for an m-dimensional set where m is the dimension of the parameter vector of the angular auto-correlation kernel. This might be nontrivial if m is large. However, for small m, the proposed method can be applied with modest increase in the computational complexity compared to that for the MUSIC algorithm.

B. The CD Source Localizer

The criterion (39) can be further simplified for CD sources. Let us define

$$\mathbf{b}(\boldsymbol{\psi}) = \int_{-(\pi/2)}^{\pi/2} \mathbf{a}(\theta)g(\theta;\boldsymbol{\psi})\, d\theta \tag{42}$$

and let $\mathbf{B}(\boldsymbol{\psi})$ be the matrix of the column vectors, $\mathbf{b}(\boldsymbol{\psi}_i), i = 1,\cdots,q$. The correlation matrix of the array is then given by

$$\mathbf{R} = \mathbf{B}(\boldsymbol{\psi})\boldsymbol{\Gamma}\mathbf{B}^H(\boldsymbol{\psi}) + \sigma_n^2\mathbf{I} \tag{43}$$

where $\boldsymbol{\Gamma}$ is a correlation matrix with the ijth component defined as $E[\gamma_i\gamma_j^*]$, and σ_n^2 is the noise variance. If the sources are uncorrelated with each other, $\boldsymbol{\Gamma}$ will be diagonal. From (43), it is seen that for CD signals the signal subspace is spanned by the eigenvectors of the correlation matrix corresponding to the q largest eigenvalues. Thus, the number of signals can be estimated as the rank of the noise-free correlation matrix. The localization criterion (39) for CD sources with the deterministic angular signal density $g(\theta;\boldsymbol{\psi})$ is given by

$$\hat{\boldsymbol{\psi}} = \arg\max_{\boldsymbol{\psi}} \frac{1}{\displaystyle\int_{-(\pi/2)}^{\pi/2}\int_{-(\pi/2)}^{\pi/2} g^*(\theta;\boldsymbol{\psi})\mathbf{a}^H(\theta)\mathbf{E}_n\mathbf{E}_n^H\mathbf{a}(\theta')g(\theta';\boldsymbol{\psi})\, d\theta\, d\theta'}. \tag{44}$$

which is found by using (9) in (39). With the definition of $\mathbf{b}(\boldsymbol{\psi}_i)$ in (42), the criterion (44) simplifies to

$$\hat{\boldsymbol{\psi}} = \arg\max_{\boldsymbol{\psi}} \frac{1}{\|\mathbf{b}^H(\boldsymbol{\psi})\mathbf{E}_n\|^2} \tag{45}$$

which is similar in form to (33). The difference is that the array manifold for CD sources is the integral of the location vector $\mathbf{a}(\theta)$ over θ, weighted by the deterministic angular signal density $g(\theta;\boldsymbol{\psi})$. To instrument the estimation, the array is calibrated with the new array manifold which is shown by $\mathbf{b}(\boldsymbol{\psi})$ and the results are saved for later use. For localization, a search step is performed on an m-dimensional space to find the maxima of (44). These maxima are the estimates of the signal parameter vectors.

C. The ID Source Localizer

For ID sources, the noise subspace is generally degenerate (i.e., equal to the zero vector) and the whole observation space is occupied by the signal components. In other words, $\mathbf{R}_s(\boldsymbol{\psi})$ in (12) is full rank. In such a case, (39) cannot be directly used. However, for several cases of practical interest, most of

the energy of the signal is concentrated in a few eigenvalues of the array correlation matrix. The number of these eigenvalues is referred to as the *effective* dimension of the signal subspace and is shown by q_e. For localization of ID sources, the number of the signal eigenvalues in the DSPE algorithm should be chosen equal to or greater than q_e. In what follows, we derive an analytical expression for the effective dimension of the signal subspace for a single uniform ID source. A similar approach has been taken in [1]. The study of a uniformly distributed source gives insight into the ID source localization problem. Later, we will explain how the DSPE method can be applied to nonuniform kernels.

Assume that an ID source with the uniform power density

$$p(\theta;\boldsymbol{\psi}) = \begin{cases} 1/(2\Delta) & \text{if } |\theta-\theta_0| \le \Delta \\ 0 & \text{otherwise} \end{cases} \tag{46}$$

is observed by a continuous linear array. That is, an observation is made at every point z in the interval $[-(L/2),(L/2)]$ where L is the array length. Using (12), it is possible to show that for a single uniform ID source, with a small extension width, the spatial cross-correlation function in a noise-free environment is given by

$$E[x^*(z)x(z')] = e^{j(2\pi/\lambda)(z'-z)\sin\theta_0} \cdot \operatorname{sinc}\left[\frac{2}{\lambda}(z'-z)\Delta\ \cos\ \theta_0\right] \tag{47}$$

where λ is the wavelength, $x(z)$ is the output of the array at the point z, and $\operatorname{sinc}(x) = (\sin\pi x/\pi x)$.

To find the effective dimension of the signal subspace, we need to perform an eigenvalue analysis of (47) by solving

$$\int_{-(L/2)}^{L/2} e^{j(2\pi/\lambda)(z-z')\sin\theta_0}\ \operatorname{sinc}\left[\frac{2}{\lambda}(z-z')\Delta\ \cos\theta_0\right] \phi_n(z')\,dz' = \mu_n\phi_n(z). \tag{48}$$

The eigenfunctions $\phi_n(z)$ are the *(modulated) angular prolate spheroidal functions* given by [13]

$$\phi_n(z) = e^{j(2\pi/\lambda)z\sin\theta_0} S_{0n}\left(c, \frac{2}{L}z\right) \tag{49}$$

where c is a parameter defined as

$$c = \pi\Delta\frac{L}{\lambda}\ \cos\ \theta_0. \tag{50}$$

The eigenvalues μ_n are equal to

$$\mu_n = 2[R_{0n}^{(1)}(c,1)]^2 \tag{51}$$

where $R_{0n}^{(1)}(c,1), n = 0,1,\cdots$, are the *radial prolate spheroidal functions* [13].

For a fixed c the radial prolate spheroidal function $R_{0n}^{(1)}(c,1)$ decreases exponentially with n. From the tables of the prolate spheroidal functions [14], it can be seen that more than 95 % of the energy is concentrated in the first $\lceil c\rceil$ eigenvalues, where $\lceil c\rceil$ indicates the smallest integer larger than c. The effective dimension of the signal subspace q_e is the number of significant eigenvalues in a noise-free environment, which we will take to be $q_e = \lceil c\rceil$. Once q_e is selected, the DSPE algorithm can be used to localize the sources.

In the above discussion, it was assumed that the source signal is observed by a continuous array with a large spatial aperture. In [15], the concept of the continuous spheroidal wave functions has been extended to discrete case. It has been shown that for a large number of discrete samples, the eigenvalues of the correlation matrix of the discrete time series can be approximated by the eigenvalues of the continuous cross-correlation function (47). In our application, if the number of sensors is large, the eigenvalues of the array correlation matrix are approximately equal to the values given in (51).

From the above discussion it is seen that the effective dimension of the signal subspace q_e is directly related to the parameter c (50). For a linear array with a half wavelength spacing, c becomes

$$c = \frac{\pi}{2}\Delta(p-1)\ \cos\theta_0. \tag{52}$$

In practice, if c is underestimated, the localization will be erroneous because some of the eigenvectors contributing to the signal subspace are not used in the localization process. When c is overestimated, no great loss of performance is observed. In such a case, the variance of the estimates is slightly reduced due to the additional noise components included in the signal subspace.

For nonuniform ID sources, an analytical expression for q_e is not available in general. However, for large SNR, q_e can be simply approximated as the number of dominant eigenvalues of the array correlation matrix. This approximation enables us to apply the DSPE algorithm to the localization of ID sources with arbitrary distribution. Using (11) in (41), $\mathbf{H}(\boldsymbol{\psi})$ simplifies to

$$\mathbf{H}(\boldsymbol{\psi}) = \int_{-(\pi/2)}^{\pi/2} \mathbf{a}(\theta)p(\theta;\boldsymbol{\psi})\mathbf{a}^H(\theta)\,d\theta. \tag{53}$$

For a uniform linear array, $\mathbf{H}(\boldsymbol{\psi})$ has a Hermitian Toeplitz form. In such a case, only p complex numbers need to be computed for each parameter vector $\boldsymbol{\psi}$.

Finally, we note that for partially correlated distributed signals (i.e., neither CD nor ID), the value of q_e lies between q and $\lceil c\rceil$. Using the number of dominant eigenvalues as the effective dimension of the signal subspace, the DSPE algorithm can be applied as well to the localization of partially correlated distributed sources.

IV. The Array Gain

Beamformers improve the array output SNR by steering a beam towards the direction of the signal. Because of the ease of implementation, these methods are practically important. However, they have relatively low resolution. In a conventional beamformer, to achieve a high resolution, a large number of sensors must be used. For point sources, increasing the number of sensors improves the array gain, defined as the ratio of the SNR at the array output to the SNR at a single sensor [16]. Assuming that the noise is spatially white and that a conventional beamformer is used, the array gain is given by

$$G_a = \frac{\mathbf{a}^H\mathbf{R}_s\mathbf{a}}{\mathbf{a}^H\mathbf{a}} \tag{54}$$

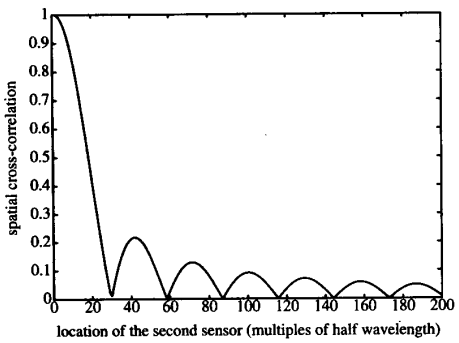

Fig. 3. Spatial cross-correlation for a uniform CD source located at 10° with an extension width 4°. (The first sensor is placed at the phase reference point.)

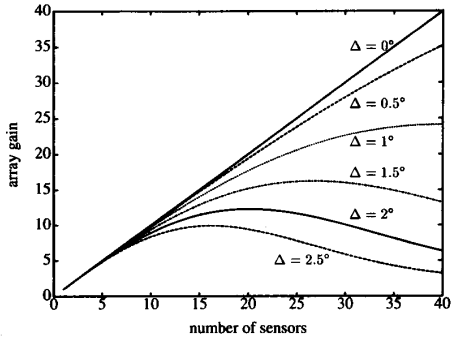

Fig. 4. Array gain for a uniform CD source for different extension widths Δ in degrees.

where $\mathbf{a}$ is the location vector of the array steered towards the direction of interest and $\mathbf{R}_s$ is the correlation matrix of the array output in a noise-free environment.

Here, we show that for distributed sources, the spatial correlation of the signal is upper bounded by an exponentially decreasing function. Then, we derive the array gain and show that it is bounded and does not increase linearly with the number of sensors.

A. The CD Source Case

Assume that the array output can be observed along a continuous linear array. If the observation at point z is shown by $x(z)$, for a CD source in a noise-free environment we have

$$x(z) = \int_{-(\pi/2)}^{\pi/2} e^{j(2\pi z/\lambda)\,\sin\,\theta} \gamma g(\theta;\boldsymbol{\psi})\, d\theta \tag{55}$$

where γ is a zero-mean complex random variable and $g(\theta;\boldsymbol{\psi})$ is the deterministic angular signal density. Assuming that the source is uniformly distributed by

$$g(\theta;\boldsymbol{\psi}) = \begin{cases} 1/(2\Delta) & \text{if } |\theta-\theta_0| \le \Delta \\ 0 & \text{otherwise} \end{cases} \tag{56}$$

the observation vector at point z can be written as

$$x(z) = \frac{\gamma}{2\Delta} \int_{\theta_0-\Delta}^{\theta_0+\Delta} e^{j(2\pi z/\lambda)\sin\theta}\, d\theta. \tag{57}$$

For a small Δ, it is straightforward to show that

$$x(z) \approx \gamma e^{j(2\pi z/\lambda)\sin\theta_0}\ \mathrm{sinc}\left(\frac{2z}{\lambda}\Delta\ \cos\ \theta_0\right). \tag{58}$$

From (58) we arrive at the following result.

Property 1: For a uniform CD source (with small extension), the spatial cross-correlation function at z_1 and z_2 in a noise-free environment is bounded by

$$|E[x(z_1)x^*(z_2)]| \le K|z_1 z_2|^{-1} \tag{59}$$

where K is a positive scalar.

An example of the correlation between two points on a linear array for a uniform CD source is depicted in Fig. 3. It is assumed that the first point is the phase reference of the array. The second point varies along the array. The envelope of the correlation function decreases as the inverse of the distance. Thus, as the aperture length of the array increases, the correlation between far-end sensors decreases. In other words, the signals at widely separated sensors cannot be coherently added to increase the SNR. This suggests that the array gain does not increase linearly with the number of sensors.

Consider a uniform linear array with half the wavelength spacing between sensors. At the position of the lth sensor (58) can be shown as

$$x_l = \gamma e^{j\pi l \sin\theta_0}\ \mathrm{sinc}(l\Delta\ \cos\ \theta_0). \tag{60}$$

Assuming that the power of the source is unity and $\theta_0 = 0$, the array gain is given by

$$G_a = \frac{1}{p}\left[\sum_{l=0}^{p-1} \mathrm{sinc}(l\Delta)\right]^2. \tag{61}$$

Note that for $\Delta = 0$ the array gain is equal to p which is the gain of a point source scenario. For $\Delta > 0$ and large p, the sum in (61) is approximated by $1/(2\Delta)$ which reveals that the array gain decreases as $1/p$. The array gain for a CD source as a function of the number of sensors p is illustrated in Fig. 4. The array gain has a maximum that depends on the extension width. Increasing the number of the sensors beyond the maximum point decreases the array gain. We have found that at the maximum point the array length $p_{\max}$ can be approximated as

$$p_{\max} \approx \frac{40}{\Delta^\circ} \tag{62}$$

where Δ° is the extension width measured in degrees.

G. The ID Source Case

From (47) we can easily arrive at the following result.

Property 2: For a uniform ID source (with small extension), the spatial cross-correlation function at z_1 and z_2 in a noise-free environment is bounded by

$$|E[x(z_1)x^*(z_2)]| \le \frac{K}{z_1 - z_2} \tag{63}$$

where K is a positive scalar.

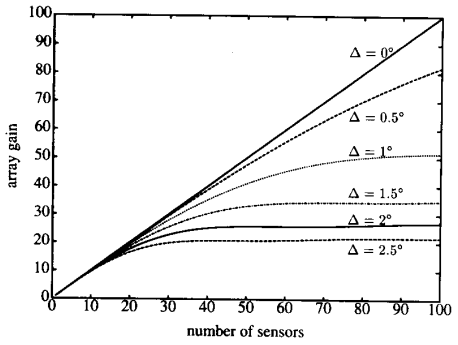

Fig. 5. Array gain for a uniform ID source for different extension widths Δ in degrees.

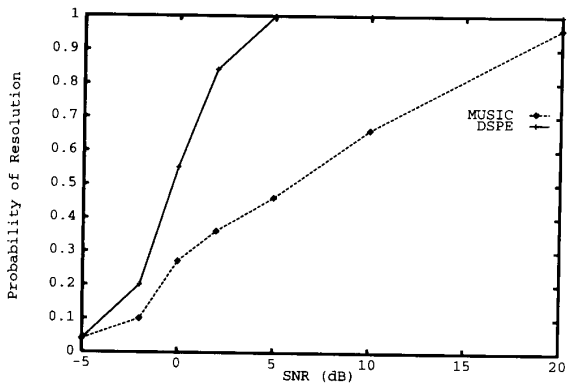

Fig. 6. Probability of resolution for the conventional MUSIC and the DSPE versus SNR.

Since the spatial correlation function decreases with distance, the array gain cannot increase linearly with the number of sensors. For a uniform linear array with half the wavelength spacing between sensors, the spatial cross-correlation function between the lth and the kth sensors is

$$E[x_l x_k^*] = e^{j\pi(l-k)\sin\theta_0}\ \mathrm{sinc}[(l-k)\Delta\ \cos\ \theta_0]. \tag{64}$$

Assuming that $\theta_0 = 0$, the array gain is given by

$$G_a = \frac{1}{p}\left[\sum_{l=0}^{p-1}\sum_{k=0}^{p-1}\mathrm{sinc}[(l-k)\Delta]\right]. \tag{65}$$

Again, it is seen that for $\Delta = 0$ we get the same result as in the point source case. With a change of variable the array gain can be represented as

$$G_a = 1 + \frac{2}{p}\sum_{r=1}^{p-1}(p-r)\,\mathrm{sinc}(r\Delta). \tag{66}$$

The array gain for an ID source is depicted in Fig. 5. Note that in this case increasing the number of sensors does not decrease the array gain. That is because for uniform ID sources the spatial cross-correlation function depends on the distance between the two observation points. Although increasing the number of sensors decreases the correlation between far-end sensors, it cannot reduce the array gain since each pair of sensors with a fixed separation have the same correlation regardless of their distance from the array reference point. However, the array gain saturates for large p as depicted in Fig. 5. For a fixed extension width, the maximum array gain for the uniform ID source is higher than that for the uniform CD source.

V. Simulation Results and Performance Comparison

A. CD Sources

We investigate a configuration with two equipower uncorrelated narrowband CD sources arriving at a uniform linear array of 20 sensors. The spacing between adjacent sensors is equal to half the wavelength at the operating frequency. The deterministic angular signal density of the ith source is given by

$$g(\theta;\boldsymbol{\psi}_i) = \frac{K_i}{1 + j\left(\dfrac{\theta-\theta_i}{\Delta_i}\right)} \qquad i = 1,2 \tag{67}$$

where K_i is a normalization factor, θ_i is the central angle of arrival, and Δ_i is the -3 dB extension width. The parameter vector in this example is $\boldsymbol{\psi}_i = (\theta_i, \Delta_i)$. The angular autocorrelation kernel for such a signal density is given by

$$p(\theta,\theta;\boldsymbol{\psi}_i) = \frac{K_i^2}{1 + \left(\dfrac{\theta-\theta_i}{\Delta_i}\right)^2} \tag{68}$$

which has a Butterworth form and is proposed in [17] as a model for noise sources. In our simulations, θ_1 and θ_2 are taken as 10 and 13° with the extension widths $\Delta_1 = 1$ and $\Delta_2 = 2°$. It is seen that the sources have a significant overlap in space.

A Monte-Carlo simulation of 50 independent runs with 50 snapshots for each trial was performed for different SNR's. The resolution performances of the conventional MUSIC and the DSPE are compared in Fig. 6. For the conventional MUSIC algorithm, the two signals are considered to be resolved when two peaks are observed in the MUSIC spectrum. For the DSPE algorithm, each source is considered detected if the estimates of θ_i and the distribution widths Δ_i are within one degree of the true values. Note that these definitions of detection tend to favor the MUSIC algorithm more than the DSPE estimator. The resolution threshold for the DSPE is about 15 dB lower than that for the conventional MUSIC algorithm.

For this source configuration, we have found the bias and the standard deviation of the estimates of the central angle in the MUSIC and the DSPE algorithms. For both sources, the estimated central DOA is biased in the conventional MUSIC algorithm and the bias cannot be decreased by increasing the SNR (see Fig. 7). The DSPE algorithm provides a smaller bias in the DOA estimation. Furthermore, the bias can be reduced by increasing the SNR. For both sources, the standard

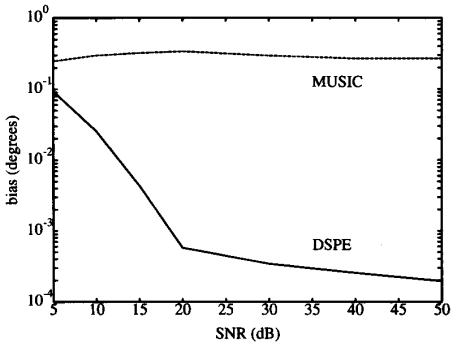

Fig. 7. Bias of estimation versus SNR for the source at 13°.

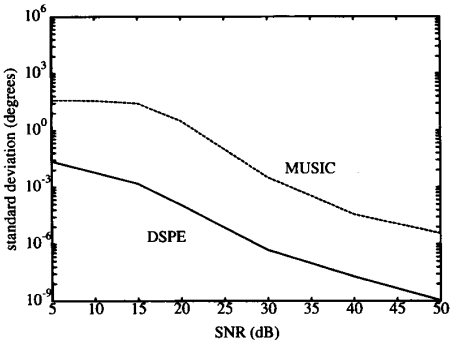

Fig. 8. Standard deviation versus SNR for the source at 13°.

deviation of the DSPE estimators is less than that for the MUSIC algorithm (see Fig. 8).

B. ID Sources

For the ID signal scenario we examine a configuration with two uniformly distributed sources with the angular power density

$$p(\theta;\boldsymbol{\psi}_i) = \begin{cases} \dfrac{1}{2\Delta_i} & \text{if } |\theta-\theta_i| \le \Delta_i, i=1,2 \\ 0 & \text{otherwise} \end{cases} \tag{69}$$

arriving at an array of 20 sensors. In our simulation, the central DOA's are selected as $\theta_1 = 8$ and $\theta_2 = 15°$ with extension widths $\Delta_1 = 1$ and $\Delta_2 = 1.5°$, respectively. The SNR is 30 dB and 100 snapshots are observed. For a single source with three degree extension width, the parameter c is smaller than 1.6. The eigenvalues of the sample correlation matrix for this scenario are shown in Fig. 9. It is seen that the first four eigenvalues dominate. The DSPE algorithm was run for this example with 16 noise eigenvectors. The DSPE spectrum is illustrated in Fig. 10. The two prominent peaks estimate the central DOA's at 7.96 and 14.90° with extension widths 1.88 and 2.80°, respectively. Note that when $\Delta = 0$ the DSPE algorithm coincides with the MUSIC algorithm. The MUSIC spectrum is the $\Delta = 0$ case in Fig. 10.

To show that higher number of eigenvalues can also be used in the DSPE algorithm, we simulated the same scenario with five eigenvectors assigned to the effective signal subspace. The

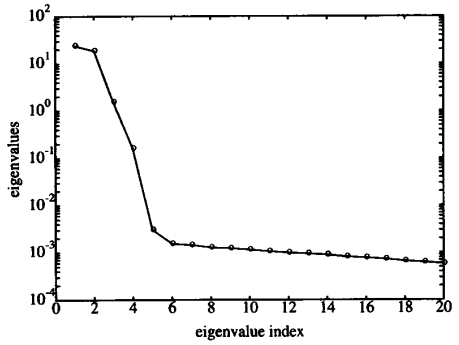

Fig. 9. Eigenvalues of a configuration with two ID signals.

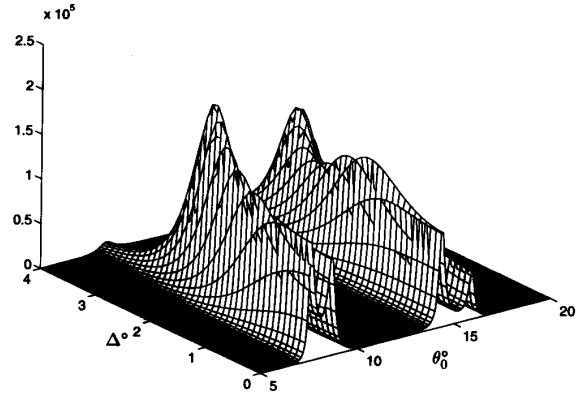

Fig. 10. Spectrum of the DSPE algorithm with the dimensionality of the effective signal subspace equal to four.

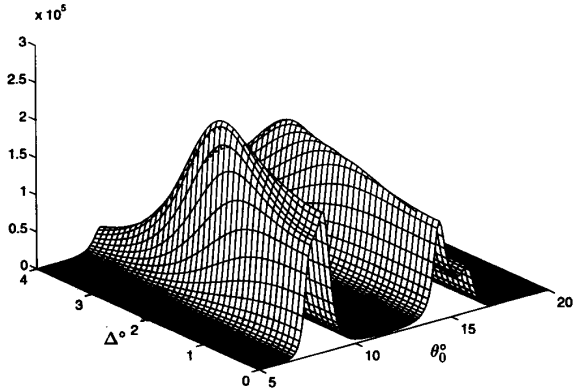

Fig. 11. Spectrum of the DSPE algorithm with the dimensionality of the effective signal subspace equal to five.

DSPE spectrum is depicted in Fig. 11. It is seen that the DSPE algorithm can still be used to locate signals. The amplitude of the spectrum at the peak points is smaller for this case. This results in a smaller resolution threshold.

VI. Summary and Conclusion

In this paper, we have discussed the problem of localizing spatially distributed sources. It has been assumed that the angular auto-correlation kernel of the source signals belongs to a parametric class. We have proposed a MUSIC-type

distributed signal parameter estimator (DSPE) that is based on minimizing a norm of the transformed noise eigenvectors in the source subspace. The method has been applied to two cases. First, we used the DSPE algorithm to localize coherently distributed (CD) signals. For the coherent distribution of signals we have shown that the new method is similar to the MUSIC algorithm with an array manifold that is the integral of the location vector weighted with the angular signal density. We have also considered incoherently distributed (ID) signals. For these signals, it has been shown that the effective dimension of the signal subspace is a function of the product of the extension width, the array aperture, wavelength, and the signal location. The DSPE algorithm is applied to ID sources using the effective dimension of the signal subspace.

Computer simulations were run to compare the new method and the conventional MUSIC algorithm. It was shown that the resolution threshold for the new method is lower than that for the MUSIC algorithm. The DSPE algorithm has a smaller bias, and unlike the MUSIC estimator, the bias can be reduced by increasing the SNR. It was also shown that the DSPE method provides a more robust estimation of the parameter vector by having a smaller standard deviation compared to the MUSIC algorithm.

Future work can be in the direction of avoiding the calibration process by using an ESPRIT-type method. In the ESPRIT algorithm it is assumed that the signal wave field is sampled with an array of perfectly matched doublets. For a distributed source, we have shown that the spatial correlation function decreases exponentially with distance. This fact should be considered in deriving an ESPRIT-type algorithm for the distributed source localization.

REFERENCES

[1] T. P. Jäntti, "The influence of extended sources on the theoretical performance of the MUSIC and ESPRIT methods: Narrow-band sources," in *Proc. IEEE Int. Conf. Acoust., Speech, Signal Processing,* San Francisco, Mar. 1992, pp. II-429–II-432.

[2] H. Kuttruff, *Room Acoustics*. Amsterdam: Elsevier Applied Science, 1991.

[3] P. F. Panter, *Communications Systems Design: Line-of-Sight and Tropo-Scatter Systems*. New York: McGraw-Hill, 1972.

[4] J. J. DeFrance, *Communications Electronics Circuits*. New York: Rinehart, 1972.

[5] D. Tholl and M. Fattouche, "Angle of arrival analysis of the indoor radio propagation channel," in *Proc. Int. Conf. Wireless Commun. (ICUPC),* Sept. 1993, pp. 79–83.

[6] R. O. Schmidt, "Multiple emitter location and signal parameter estimation," *IEEE Trans. Antenn. Propagat.,* vol. AP-34, pp. 276–280, Mar. 1986.

[7] R. Roy and T. Kailath, "ESPRIT—Estimation of signal parameters via rotational invariance techniques," *IEEE Trans. Acoust., Speech, Signal Processing,* vol. 37, pp. 984–995, July 1989.

[8] M. Wax, "On unique localization of constrained-signals sources," *IEEE Trans. Signal Processing,* vol. 40, pp. 1542–1547, June 1992.

[9] Y. Meng, K. M. Wong, and Q. Wu, "Estimation of the direction of arrival of spread sources in sensor array processing," in *Proc. Int. Conf. Signal Processing,* Beijing, China, Oct. 1993, pp. 430–434.

[10] Q. Wu, K. M. Wong, Y. Meng, and W. Read, "DOA estimation of point and scattered sources—Vec-MUSIC," in *7th SP Workshop Statistical Signal Array Processing,* Québec City, Canada, June 1994, pp. 365–368.

[11] S. Valaee, P. Kabal, and B. Champagne, "Localization of distributed sources," in *14th GRETSI Symp. Signal Image Processing,* Juan-les-Pins, France, Sept. 1993, pp. 289–292.

[12] B. Champagne, M. Eizenman, and S. Pasupathy, "Factorization properties of optimum space-time processors in nonstationary environments," *IEEE Trans. Acoust., Speech, Signal Processing,* vol. 38, pp. 1853–1869, Nov. 1990.

[13] D. Slepian and H. O. Pollak, "Prolate spheroidal wave functions, Fourier analysis and uncertainty—I," *Bell Syst. Tech. J.,* vol. 40, pp. 43–64, 1961.

[14] D. Slepian and E. Sonnenblick, "Eigenvalues associated with prolate spheroidal wave functions of zero order," *Bell Syst. Tech. J.,* vol. 44, pp. 1745–1759, 1965.

[15] D. Slepian, "Prolate spheroidal wave functions, Fourier analysis and uncertainty—V: The discrete case," *Bell Syst. Tech. J.,* vol. 57, pp. 1371–1430, 1978.

[16] D. H. Johnson and D. E. Dudgeon, *Array Signal Processing: Concepts and Techniques*. Englewood Cliffs, NJ: Prentice-Hall, 1993.

[17] S. Haykin, Ed., *Array Signal Processing*. Englewood Cliffs, NJ: Prentice-Hall, 1985.

Shahrokh Valaee was born in Tabriz, Iran. He received the B.Sc. and M.Sc. degrees from Tehran University, Tehran, Iran, and the Ph.D. from McGill University, Montréal, Canada, all in electrical engineering.

While at McGill, he was a research and senior teaching assistant in communications and signal processing courses. He also has three years of experience in designing PABX systems. Presently, he is a research associate at INRS, Université du Québec, working on congestion control in B-ISDN.

His research interests include detection and estimation, modeling and order selection, spectrum estimation and harmonic retrieval, beamforming and array processing, and recently ATM networks.

Benoit Champagne (S'87–M'89) was born in Joliette, Quebec, Canada on January 13, 1961. He received the B.Ing. degree in engineering physics from the Ecole Polytechnique of Montréal in 1983, the M.Sc. degree in physics from the University of Montréal in 1985, and the Ph.D. degree in electrical engineering from the University of Toronto in 1990.

In June 1990, he joined INRS-Telecommunications, Université du Québec, where he is now an associate professor. Since September 1994, he has also been Adjunct Professor of Electrical Engineering at McGill University. His current research interests are in the area of statistical signal processing, with particular emphasis on array processing and adaptive filtering.

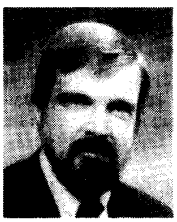

Peter Kabal (S'70–M'75) received the B.A.Sc., M.A.Sc., and Ph.D. degrees in electrical engineering from the University of Toronto, Toronto, Ontario, Canada.

He is a Professor in the Department of Electrical Engineering at McGill University, Montréal, Quebec, Canada, and a Visiting Professor at INRS (a research institute affiliated with the Université du Québec), Verdun, Québec. From September 1982 to September 1983, he was a full-time consultant to the Speech Communications Group at Bell-Northern Research, Verdun, Québec. From September 1987 to June 1988, he spent a sabbatical year as a Visiting Professor at the University of California, Santa Barbara. His current research interests focus on signal processing as applied to speech coding, adaptive filtering, and data transmission.